ACS Energy LETTERS

Cite This: ACS Energy Lett. 2018, 3, 193−198

LETTER

Insights into the Low Overpotential Electroreduction of CO_2 to CO on a Supported Gold Catalyst in an Alkaline Flow Electrolyzer

Sumit Verma,[†,‡] Yuki Hamasaki,[‡,#] Chaerin Kim,[‡,#] Wenxin Huang,[‡,#] Shawn Lu,[†] Huei-Ru Molly Jhong,[†,‡] Andrew A. Gewirth,[§,‡] Tsuyohiko Fujigaya,[*,‡,#] Naotoshi Nakashima,[*,‡,#] and Paul J. A. Kenis[*,†,‡]

[†]Department of Chemical & Biomolecular Engineering, University of Illinois at Urbana−Champaign, 600 South Mathews Avenue, Urbana, Illinois 61801, United States

[‡]International Institute for Carbon Neutral Energy Research (WPI-I2CNER), Kyushu University, 744 Moto-oka, Nishi-ku, Fukuoka 819-0395, Japan

[#]Department of Applied Chemistry, Kyushu University, 744 Moto-oka, Nishi-ku, Fukuoka 819-0395, Japan

[§]Department of Chemistry, University of Illinois at Urbana−Champaign, 505 South Mathews Avenue, Urbana, Illinois 61801, United States

Supporting Information

ABSTRACT: **Cost competitive electroreduction of CO_2 to CO requires electrochemical systems that exhibit partial current density (j_{CO}) exceeding 150 mA cm^{-2} at cell overpotentials ($|\eta_{cell}|$) less than 1 V. However, achieving such benchmarks remains difficult. Here, we report the electroreduction of CO_2 on a supported gold catalyst in an alkaline flow electrolyzer with performance levels close to the economic viability criteria. Onset of CO production occurred at cell and cathode overpotentials of just −0.25 and −0.02 V, respectively. High j_{CO} (~99, 158 mA cm^{-2}) was obtained at low $|\eta_{cell}|$ (~0.70, 0.94 V) and high CO energetic efficiency (~63.8, 49.4%). The performance was stable for at least 8 h. Additionally, the onset cathode potentials, kinetic isotope effect, and Tafel slopes indicate the low overpotential production of CO in alkaline media to be the result of a pH-independent rate-determining step (i.e., electron transfer) in contrast to a pH-dependent overall process.**

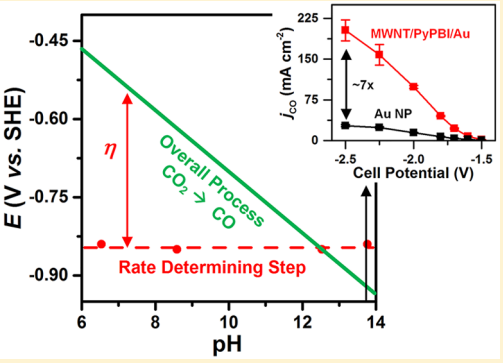

Carbon dioxide (CO_2) levels in the earth's atmosphere has been on a constant rise in the past few decades, with the daily average value exceeding and staying above the 400 ppm mark in 2016 for the first time in recorded human history.[1] This rise in atmospheric CO_2 levels has been correlated to the increase in global mean temperature anomalies and the associated climate change effects.[2] Thus, developing cost-effective technologies that can mitigate, capture, or utilize excess anthropogenic CO_2 emissions remains a grand challenge for the 21st century.[3] The electroreduction of CO_2 to value added C_1−C_2 chemicals [e.g., formic acid (HCOOH), carbon monoxide (CO), methanol, ethanol, ethylene, etc.] using renewable energy could be one approach for utilizing and reducing the excess CO_2 emissions.[4,5] However, prior technoeconomic analysis suggests that out of the myriad of C_1−C_2 chemicals that can be obtained via the electroreduction of CO_2, producing CO and HCOOH seems to be the most viable as the process can become cost competitive with the existing industrial methods to manufacture the same.[6,7]

Starting with the early work of Hori et al.,[8,9] many studies have focused on the development of active, selective, and stable catalysts as well as electrolytes for the electroreduction of CO_2.[10−12] In particular, for the electroreduction of CO_2 to CO, gold (Au)[13−17] and silver (Ag)[18−23] have been shown to be two of the most active catalytic materials. Yet, even after almost two decades of research, achieving high levels of activity [partial current density for CO (j_{CO}) > 150 mA cm^{-2}] at low cell overpotentials ($|\eta_{cell}|$ < 1 V), a criterion required for the economic viability of the CO_2 electroreduction process,[6,24] remains challenging.[25] Such a behavior can primarily be attributed to a combination of (1) low solubility of CO_2 in

Received: November 7, 2017
Accepted: December 18, 2017
Published: December 18, 2017

DOI: 10.1021/acsenergylett.7b01096
ACS Energy Lett. 2018, 3, 193−198

aqueous solutions (~35 mM at 298 K and 1 atm pressure)[26] causing mass transport limitations when using dissolved CO_2 as the reactant and (2) a high activation barrier associated with the formation of the rate-determining CO_2^- radical.[27,28] While the use of gas diffusion layer (GDL) electrode-based flow electrolyzers could be a reactor engineering approach to circumvent CO_2 mass transport limitations by supplying a continuous CO_2 stream at the electrode−electrolyte interface,[29,30] electrolyte engineering approaches such as the use of imidazolium-based ionic liquids,[31] large cations,[32,33] and alkaline media are alternative methods to lower overpotentials and improve activity.[34,35] However, the mechanism behind the beneficial effects of such electrolytes (especially alkaline media/high pH) is still poorly understood.

In this work, we report the active, selective, and stable electroreduction of CO_2 to CO using Au nanoparticles supported on poly(2,2′-(2,6-pyridine)-5,5′-bibenzimidazole) polymer (PyPBI) wrapped multiwall carbon nanotubes (MWNTs) as the cathode catalyst (MWNT/PyPBI/Au). The MWNT/PyPBI/Au catalyst was further utilized to provide new insights into the reaction mechanism and durability of CO_2 electroreduction at high electrolyte pH. Previously, we reported similar catalysts, i.e., platinum (diameter < 5 nm)[36,37] and Au nanoparticles (diameter 1−20 nm),[38] supported on PyPBI wrapped MWNTs for the oxygen (O_2) and CO_2 electroreduction reactions, respectively. Because catalyst nanoparticle size is known to affect the electroreduction of CO_2 to CO, with a dramatic enhancement in the mass activity being observed when using Ag or Au nanoparticles with diameter less than 10 nm,[16,17,23] we refined our synthesis method (i.e., lowered the target Au loading on the MWNT/PyPBI support from ~50% by weight in ref 38 to ~15% by weight in this work)[39] to deposit 3.4 ± 1.3 nm Au nanoparticles on the PyPBI wrapped MWNT support (Figure 1a,b). The actual Au content in MWNT/PyPBI/Au was found to be ~18% by weight (Figure 1c). The MWNT/PyPBI/Au catalyst was then deposited onto a GDL via an automated airbrush method,[40] with a final loading of 1.0 ± 0.1 mg cm^{-2} (Au ~ 0.18 mg cm^{-2}). The electrochemical characterization of the MWNT/PyPBI/Au coated GDL was performed in a flow electrolyzer (Figure S1),[29] with a CO_2 flow rate (F_{CO_2}) of 17 sccm and an electrolyte flow rate of 0.5 mL min^{-1}. The cathodic CO_2 electroreduction was coupled to the anodic O_2 evolution on an iridium oxide (IrO_2) coated GDL to lower $|\eta_{cell}|$.[41]

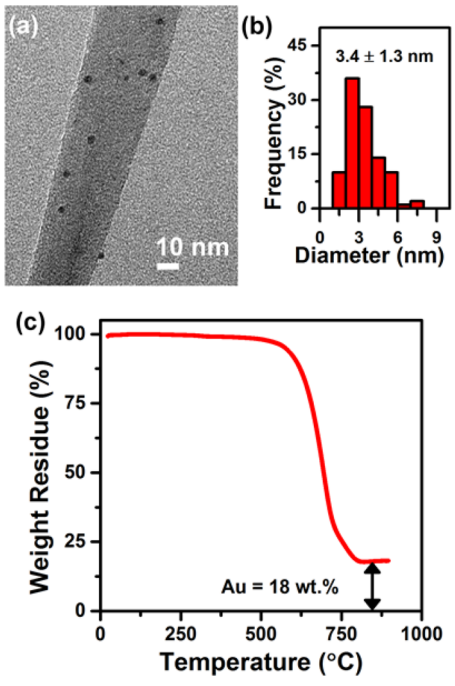

Figure 1. (a) Representative transmission electron microscopy image, (b) size histogram (100 particles), and (c) thermogravimetric analysis (10 °C minute^{-1} in air) for the as-synthesized MWNT/PyPBI/Au catalyst.

The MWNT/PyPBI/Au cathode in combination with the IrO_2 anode and 2.0 M KOH electrolyte shows an onset cell, cathode potential of just −1.50 V (η_{cell} ~ −0.25 V) and −0.04 V vs RHE [cathode overpotential ($\eta_{cathode}$) ~ −0.02 V], respectively, for the electroreduction of CO_2 to CO (Figure 2a,b; see section S2.2, Table S1 for η_{cell} and $\eta_{cathode}$ calculations). The onset potential (cell or cathode) is defined as the least negative potential (cell or cathode) at which CO is first observed in the gas chromatograph with a signal-to-noise ratio greater than 3. The electrochemical system also exhibits high activity at low cell and cathode potentials with j_{CO} as high as, for example, 99 and 158 mA cm^{-2} being obtained at a cell potential of only −2.00 and −2.25 V, and a cathode potential of just −0.42 and −0.55 V vs RHE (Figure 2b). The values correspond to a high mass activity for CO (548.8 and 877.5 A g_{Au}^{-1}) at high energetic efficiencies (63.8 and 49.4%) (Table 1). The MWNT/PyPBI/Au catalyst exhibits a 2−5× improvement in total current density (j_{Total}) and 3.5−7× improvement in j_{CO} over commercially available surfactant free Au nanoparticles (size, <100 nm; loading = 0.18 ± 0.02 mg cm^{-2}) (Figure 2a,b). Meanwhile, the MWNT/PyPBI support (loading = 1.0 ± 0.01 mg cm^{-2}) does not show any activity toward CO production (Figure 2b). The improved performance can be attributed to a combination of (i) small Au particles with a narrow size distribution, (ii) high electrochemically active surface area of the MWNT/PyPBI/Au catalyst due to the unique ability of the pyridine-containing PyPBI to provide nucleation sites for the deposition and growth of the Au nanoparticles, as well as (iii) high electrical conductivity of the MWNT support.[16,17,23,36−38] To the best of our knowledge, these results represent the lowest onset cell and cathode potential along with some of the highest j_{CO}, mass activity at low cell and cathode potentials for the electroreduction of CO_2 to CO (see Figure S2 for a comparison with the literature).

Electrolyte (KOH) concentration was found to play a crucial role in the process with a 1.5−2× improvement in j_{CO} being observed when moving from 1.0 to 2.0 M KOH (Figure 2c). However, the improvement in j_{CO} on further increasing the concentration to 3.0 M KOH was less significant, especially at cathode potentials > −0.7 V vs RHE. The electrolyte anion/pH was found to be important as well with a less negative onset cathode potential (hence low $|\eta_{cathode}|$) and a higher j_{CO} at low $|\eta_{cathode}|$ being observed when using KOH in comparison to K_2CO_3, $KHCO_3$, or KCl (Figure 2d and Table 2). Previously, we demonstrated a similar lowering of $|\eta_{cathode}|$ and an improvement in j_{CO} on increasing the electrolyte pH and changing the anion from Cl^- to HCO_3^- and OH^-, for CO_2 electroreduction on Ag nanoparticle coated GDLs.[33−35] The results were rationalized on the basis of (1) slower kinetics of the parasitic H_2 evolution reaction at high

DOI: 10.1021/acsenergylett.7b01096
ACS Energy Lett. 2018, 3, 193−198

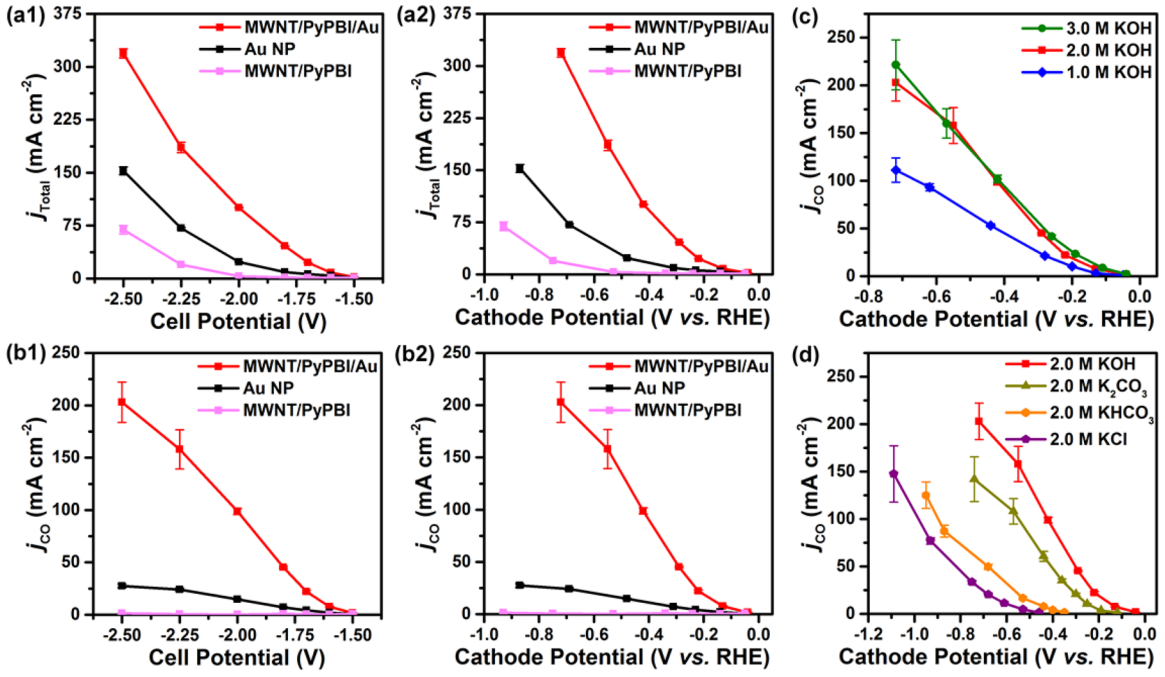

Figure 2. (a) Total current density (j_{Total}) and (b) partial current density for CO (j_{CO}) as a function of the cell, cathode potential when using MWNT/PyPBI/Au, MWNT/PyPBI, and commercially available Au nanoparticles (Au NP) as the cathode catalyst (electrolyte: 2.0 M KOH), as well as j_{CO} as a function of the cathode potential for the MWNT/PyPBI/Au cathode catalyst when using (c) three different concentrations of KOH and (d) 2.0 M KOH, K_2CO_3, $KHCO_3$, KCl as the electrolyte. Anode is IrO_2.

Table 1. Cathode Potential, Faradaic Efficiency (FE_{CO}), Mass Activity, and Energetic Efficiency (EE_{CO}) for the Electroreduction of CO_2 to CO on a MWNT/PyPBI/Au Cathode Catalyst, at Different Cell Potentials[a]

cell potential (V)	cathode potential (V vs RHE)	Faradaic efficiency (FE_{CO}) (%)	mass activity for CO (A g_{Au}^{-1})	energetic efficiency (EE_{CO}) (%)
−1.50	−0.04	73.8	9.6	61.4
−1.60	−0.13	92.4	42.5	73.2
−1.70	−0.22	98.3	123.2	74.1
−1.80	−0.29	98.2	251.0	70.4
−2.00	−0.42	98.2	548.8	63.8
−2.25	−0.55	85.0	877.5	49.4
−2.50	−0.72	63.6	1127.5	33.3

[a]Anode, IrO_2; electrolyte, 2.0 M KOH. See section S2.3 for EE_{CO} calculations.

Table 2. Onset Cathode Potential for the Electroreduction of CO_2 to CO, when Using Ag Nanoparticles; MWNT/PyPBI/Au as the Cathode Catalyst; and 2.0 M KOH, K_2CO_3, $KHCO_3$, or KCl as the Electrolyte (Anode: IrO_2)

		onset cathode potential for CO (V)			
		Ag nanoparticles[34]		MWNT/PyPBI/Au	
electrolyte	pH	vs RHE	vs SHE	vs RHE	vs SHE
2.0 M KOH	13.77	−0.13	−0.94	−0.04	−0.84
2.0 M K_2CO_3	12.53	−0.23[a]	−0.97[a]	−0.12	−0.85
2.0 M $KHCO_3$	8.59	−0.46	−0.97	−0.35	−0.85
2.0 M KCl	6.54	−0.60	−0.99	−0.46	−0.84

[a]Values originally not reported in ref 34 but acquired for this work under identical experimental conditions to complete the data set.

pH[35,42] and (2) the ability of anions (Cl^-, sulfonates, etc.) to specifically adsorb to the catalytic Ag surface and destabilize the rate-determining CO_2^- radical.[34] While the improvement in j_{CO} at low $|\eta_{cathode}|$ in the case of the MWNT/PyPBI/Au catalyst with a KOH electrolyte can still be explained by inhibited H_2 evolution in alkaline media, the shift in onset potential for CO is hard to explain using the specific anion adsorption effect. This is because the potential of zero charge (pzc) for Au (~0.2 V vs SHE) is much more positive than that for Ag (−0.5 to −0.8 V vs SHE)[43] as well as the operating potentials for CO_2 electroreduction (cathode potentials < −0.8 V vs SHE, Table 2), suggesting that specific anion adsorption might be relevant for Ag but should not be a factor for Au.

A closer look at the onset cathode potentials for CO production on MWNT/PyPBI/Au (this work) and Ag nanoparticles (from the literature)[34] shows that for a given catalytic material, the values were similar for all the electrolytes/pH versus SHE but different versus RHE (Table 2). Note that the onset cathode potentials were nearly identical with or without *iR* correction (Table S1 in the Supporting Information). Revisiting the potential (E)−pH (Pourbaix) diagrams for elementary electrochemical steps, i.e., electron transfer and concerted proton electron transfer (Figures S3), indicates that the potential remaining constant on the SHE scale irrespective of pH is the characteristic of an electron-transfer step.[44,45] As the onset potential for a product is determined by the rate-determining step (rds), we hypothesize that the rds for the electroreduction of CO_2 to CO should be electron transfer in contrast to the commonly assumed concerted proton electron transfer for computational (density functional theory) studies of CO_2 electroreduction.[46] To further verify our hypothesis, we performed a kinetic isotope effect study (section S2.6). If protons were involved in the rds, then differences in activity for CO production should be observed when using protonated versus deuterated electrolytes.[47−50] However, the Tafel plots for CO formation in both the protonated and deuterated electrolytes were found to be

DOI: 10.1021/acsenergylett.7b01096
ACS Energy Lett. 2018, 3, 193−198

nearly identical (Figure S4), indicating that protons are not involved in the rds. Hence, electron transfer should indeed be the rate-determining step.

The elementary steps describing the electroreduction of CO_2 to CO on transition-metal surfaces under neutral to alkaline pH can be written as follows:[8,51]

$$CO_2 + e^- + [*] \rightarrow CO_2^-(ads) \quad (1)$$

$$CO_2^-(ads) + H_2O \rightarrow COOH(ads) + OH^- \quad (2)$$

$$COOH(ads) + e^- \rightarrow COOH^-(ads) \quad (3)$$

$$COOH^-(ads) \rightarrow CO(ads) + OH^- \quad (4)$$

$$CO(ads) \rightarrow CO(g) + [*] \quad (5)$$

where [*] denotes an active site. Of the 5 steps, only eqs 1 and 3 represent an electron-transfer step. If eq 1 or 3 were the rds, the Tafel slope should be 116 and 39 mV decade^{-1}, respectively (section S2.7). The Tafel slopes for all the electrolytes studied in this work were between 115 and 133 mV decade^{-1} in the kinetically controlled regime (Figure 3a), indicating the rate-determining step to be eq 1. In contrast, the overall electroreduction of CO_2 to CO is pH-dependent, resulting in a lower $|\eta_{cathode}|$ and hence a positive shift in onset potentials at high pH (Figure 3b). Note, that the equilibrium potential associated with eq 1, i.e., the formation of CO_2^-(ads) (−1.9 V vs SHE)[27] is much more negative than the onset potential of −0.84 to −0.85 V vs SHE and −0.94 to −0.99 V vs SHE for CO production on MWNT/PyPBI/Au and Ag nanoparticles, respectively. The large difference can be interpreted according to a hypothesis originally proposed by Hori and co-workers, i.e., the stabilization of CO_2^-(ads) on transition metals is possible at potentials more positive than −1.9 V vs SHE because of the back-donation of electrons from the highest occupied d orbital of the metallic catalyst to the lowest unoccupied antibonding orbital of CO_2^-(ads).[8,9] Different materials can facilitate this back-donation to a different extent, thus determining their catalytic properties. Interestingly, we do observe this phenomenon in our experiments in terms of a different onset potential for CO production on MWNT/PyPBI/Au (more positive value, hence better catalyst) in comparison to Ag nanoparticles (Table 2 and Figure 3b).

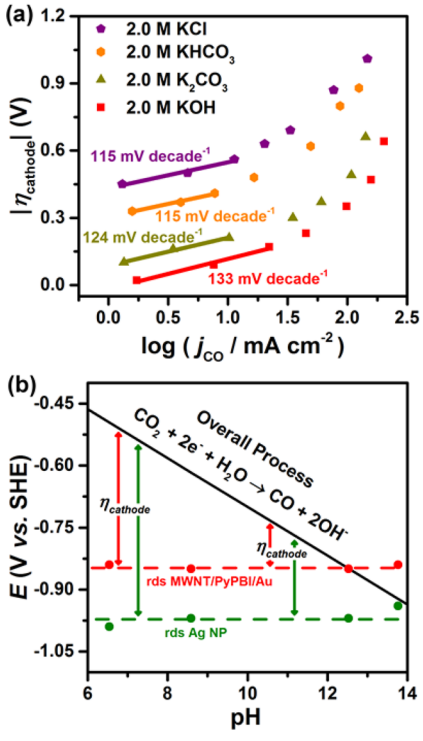

Figure 3. (a) Tafel slopes for the electroreduction of CO_2 to CO when using 2.0 M KOH, K_2CO_3, $KHCO_3$, or KCl as the electrolyte. Cathode, MWNT/PyPBI/Au; anode, IrO_2. (b) *E*−pH (Pourbaix) diagram for the electroreduction of CO_2 to CO depicting pH independence of the onset cathode potentials [hence, rate-determining step (rds)] vs pH dependence of the overall process. Note, rds MWNT/PyPBI/Au and rds Ag NP denote the rate-determining step for the MWNT/PyPBI/Au and Ag nanoparticle catalyst, respectively.

Next, we investigated the durability of the MWNT/PyPBI/Au coated GDL using a 2.0 M KOH electrolyte and an IrO_2 anode in a flow electrolyzer. Electrochemical experiments were performed at a constant cathode potential of −1.45 V vs Ag/AgCl (−0.44 V vs RHE) for 8 h to achieve realistic operating conditions of j_{CO} > 100 mA cm^{-2} and FE_{CO} > 90%. During preliminary experiments using F_{CO_2} = 17 sccm, we observed electrolyte flooding through the GDL leading to blockage of the CO_2 feed line due to carbonate precipitation (demonstrated by sharp fluctuations in j_{Total} in Figure S5a and visible precipitates in Figure S5b). Increasing F_{CO_2} to 75 sccm eliminated this problem as evidenced by the absence of sharp j_{Total} fluctuations (Figure S5). The result can be attributed to a better pressure balance at the gas−electrode−electrolyte interface. However, at the end of the experiment, traces of carbonate precipitate (that can impede the transport of CO_2 and electrons to the catalytic sites) were observed on the macroporous layer of the GDL. Hence, to avoid degradation effects related to electrolyte flooding and carbonate precipitation, and thus truly assess the durability of the MWNT/PyPBI/Au coated GDL, we repeated the experiment at F_{CO_2} = 75 sccm with a wash of the macroporous layer of the GDL with deionized (DI) water at intervals of 2.5 h. The electrochemical system showed considerable durability during the test, with FE_{CO} remaining nearly constant over the 8 h period (Figure 4a). j_{Total} was relatively stable with the value changing from ∼111 mA cm^{-2} at the end of 1 h to ∼103 mA cm^{-2} at the end of 8 h (∼7% drop). Interestingly, the FE_{CO} improved from 86% to 90% after the first wash of the GDL with DI water (Figure 4a), indicating that carbonate precipitation indeed affects electrochemical performance. The MWNT/PyPBI/Au catalyst (final Au size = 3.6 ± 1.4 nm) was also stable during the 8 h run (Figure 4b,c).

In summary, we have shown that an electrochemical system comprising a MWNT/PyPBI/Au-coated GDL cathode, IrO_2-coated GDL anode, and 2.0 M KOH electrolyte exhibits high activity for the electroreduction of CO_2 to CO at low overpotentials. Specifically, the electrochemical system exhibits an onset cell potential of just −1.50 V, an onset cathode potential of just −0.04 V vs RHE, and j_{CO} as high as 99 and 158 mA cm^{-2} at corresponding energetic efficiencies for CO of 63.8 and 49.4%. The electrochemical system also showed considerable durability over 8 h. While the results reported here seem promising, future work should focus on extending the durability of the electrochemical system to >3000 h if one were to demonstrate true industrial relevance. An issue of

DOI: 10.1021/acsenergylett.7b01096
ACS Energy Lett. 2018, 3, 193−198

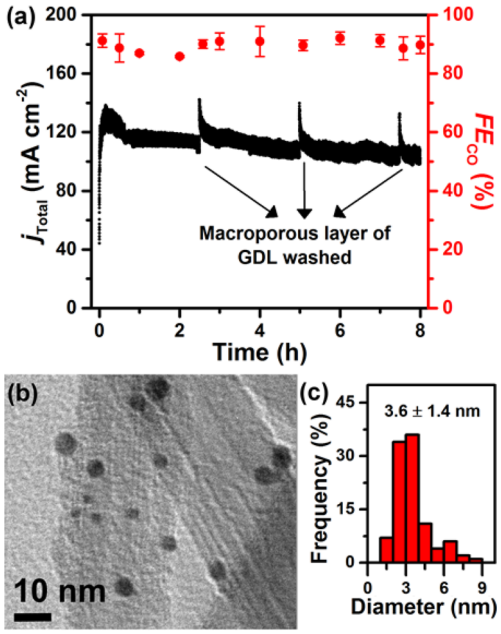

Figure 4. (a) Variation in the total current density (j_{Total}) and Faradaic efficiency for CO (FE_{CO}) with time at a constant cathode potential of −0.44 V vs RHE. Cathode, MWNT/PyPBI/Au; anode, IrO_2; electrolyte, 2.0 M KOH. (b) Representative transmission electron microscopy image and (c) size histogram (100 particles) for the MWNT/PyPBI/Au catalyst after 8 h.

special concern would be developing methods that can eliminate carbonate formation and/or regenerate the spent electrolyte in alkaline CO_2 electroreduction systems. Possible solutions include but are not limited to (i) utilizing an anion exchange membrane electrolyzer or (ii) reacting the formed potassium carbonate with slaked lime ($Ca(OH)_2$) to regenerate the KOH in solution and precipitate out calcium carbonate. However, additional technoeconomic analyses need to be performed to understand the cost effectiveness and energy efficiency of such proposed systems. From a fundamental reaction mechanism perspective, we used a combination of the onset cathode potential data, kinetic isotope effect, and Tafel slopes to show that the rate-determining step for the electroreduction of CO_2 to CO is a pH-independent electron-transfer step involving the formation of the adsorbed CO_2^- radical. As a result, increasing electrolyte pH might be an effective way of lowering the high $|\eta_{cathode}|$ requirement.

■ ASSOCIATED CONTENT

Supporting Information

The Supporting Information is available free of charge on the ACS Publications website at DOI: 10.1021/acsenergylett.7b01096.

Experimental section, details of the Faradaic efficiency, overpotential, energetic efficiency calculations, *iR* corrected data, comparison of the results reported in this work versus the literature, theoretical Pourbaix diagrams for electron transfer and concerted proton electron transfer, kinetic isotope effect analysis, Tafel slope calculations, and durability testing for different CO_2 flow rates (PDF)

■ AUTHOR INFORMATION

Corresponding Authors

*E-mail: fujigaya.tsuyohiko.948@m.kyushu-u.ac.jp.
*E-mail: nakashima.naotoshi.614@m.kyushu-u.ac.jp.
*E-mail: kenis@illinois.edu.

ORCID

Andrew A. Gewirth: 0000-0003-4400-9907
Paul J. A. Kenis: 0000-0001-7348-0381

Notes

The authors declare no competing financial interest.

■ ACKNOWLEDGMENTS

The authors gratefully acknowledge financial support from the International Institute for Carbon Neutral Energy Research (WPI-I2CNER), sponsored by the Japanese Ministry of Education, Culture, Sports, Science and Technology, and from a Dow Chemical Company graduate fellowship to S.V. TGA was carried out in part in the Frederick Seitz Materials Research Laboratory Central Research Facilities, University of Illinois.

■ REFERENCES

(1) Ussiri, D. A.; Lal, R. Introduction to Global Carbon Cycling: An Overview of the Global Carbon Cycle. In *Carbon Sequestration for Climate Change Mitigation and Adaptation*; Springer: Cham, Switzerland, 2017.

(2) Hansen, J.; Kharecha, P.; Sato, M.; Masson-Delmotte, V.; Ackerman, F.; Beerling, D. J.; Hearty, P. J.; Hoegh-Guldberg, O.; Hsu, S. L.; Parmesan, C.; Rockstrom, J.; Rohling, E. J.; Sachs, J.; Smith, P.; Steffen, K.; Van Susteren, L.; von Schuckmann, K.; Zachos, J. C. Assessing "Dangerous Climate Change": Required Reduction of Carbon Emissions to Protect Young People, Future Generations and Nature. *PLoS One* **2013**, *8*, e81648.

(3) Chu, S.; Majumdar, A. Opportunities and Challenges for a Sustainable Energy Future. *Nature* **2012**, *488*, 294−303.

(4) Herron, J. A.; Kim, J.; Upadhye, A. A.; Huber, G. W.; Maravelias, C. T. A General Framework for the Assessment of Solar Fuel Technologies. *Energy Environ. Sci.* **2015**, *8*, 126−157.

(5) Jhong, H. R. M.; Ma, S.; Kenis, P. J. A. Electrochemical Conversion of CO_2 to Useful Chemicals: Current Status, Remaining Challenges, and Future Opportunities. *Curr. Opin. Chem. Eng.* **2013**, *2*, 191−199.

(6) Verma, S.; Kim, B.; Jhong, H. R. M.; Ma, S.; Kenis, P. J. A. A Gross-Margin Model for Defining Technoeconomic Benchmarks in the Electroreduction of CO_2. *ChemSusChem* **2016**, *9*, 1972−1979.

(7) *Carbon Dioxide Utilization. Electrochemical Conversion of CO_2 − Opportunities and Challenges*; Position Paper 07-2011; Det Norske Veritas (DNV): Høvik, Norway, 2011.

(8) Hori, Y. Electrochemical CO_2 Reduction on Metal Electrodes. In *Modern Aspects of Electrochemistry*; Springer: New York, 2008.

(9) Hori, Y.; Wakebe, H.; Tsukamoto, T.; Koga, O. Electrocatalytic Process of CO Selectivity in Electrochemical Reduction of CO_2 at Metal-Electrodes in Aqueous-Media. *Electrochim. Acta* **1994**, *39*, 1833−1839.

(10) Qiao, J. L.; Liu, Y. Y.; Hong, F.; Zhang, J. J. A Review of Catalysts for the Electroreduction of Carbon Dioxide to Produce Low-Carbon Fuels. *Chem. Soc. Rev.* **2014**, *43*, 631−675.

(11) Kumar, B.; Brian, J. P.; Atla, V.; Kumari, S.; Bertram, K. A.; White, R. T.; Spurgeon, J. M. New Trends in the Development of Heterogeneous Catalysts for Electrochemical CO_2 Reduction. Catal. *Catal. Today* **2016**, *270*, 19−30.

(12) Lu, Q.; Jiao, F. Electrochemical CO_2 Reduction Electrocatalyst, Reaction Mechanism, and Process Engineering. *Nano Energy* **2016**, *29*, 439−456.

(13) Cao, Z.; Kim, D.; Hong, D. C.; Yu, Y.; Xu, J.; Lin, S.; Wen, X. D.; Nichols, E. M.; Jeong, K.; Reimer, J. A.; Yang, P. D.; Chang, C. J.

DOI: 10.1021/acsenergylett.7b01096
ACS Energy Lett. 2018, 3, 193−198

A Molecular Surface Functionalization Approach to Tuning Nanoparticle Electrocatalysts for Carbon Dioxide Reduction. *J. Am. Chem. Soc.* **2016**, *138*, 8120−8125.
(14) Chen, Y. H.; Li, C. W.; Kanan, M. W. Aqueous CO_2 Reduction at Very Low Overpotential on Oxide-Derived Au Nanoparticles. *J. Am. Chem. Soc.* **2012**, *134*, 19969−19972.
(15) Huan, T. N.; Prakash, P.; Simon, P.; Rousse, G.; Xu, X.; Artero, V.; Gravel, E.; Doris, E.; Fontecave, M. CO_2 Reduction to CO in Water: Carbon Nanotube-Gold Nanohybrid as a Selective and Efficient Electrocatalyst. *ChemSusChem* **2016**, *9*, 2317−2320.
(16) Mistry, H.; Reske, R.; Zeng, Z. H.; Zhao, Z. J.; Greeley, J.; Strasser, P.; Cuenya, B. R. Exceptional Size-Dependent Activity Enhancement in the Electroreduction of CO_2 over Au Nanoparticles. *J. Am. Chem. Soc.* **2014**, *136*, 16473−16476.
(17) Zhu, W. L.; Michalsky, R.; Metin, O.; Lv, H. F.; Guo, S. J.; Wright, C. J.; Sun, X. L.; Peterson, A. A.; Sun, S. H. Monodisperse Au Nanoparticles for Selective Electrocatalytic Reduction of CO_2 to CO. *J. Am. Chem. Soc.* **2013**, *135*, 16833−16836.
(18) Ma, S.; Lan, Y.; Perez, G. M. J.; Moniri, S.; Kenis, P. J. A. Silver Supported on Titania as an Active Catalyst for Electrochemical Carbon Dioxide Reduction. *ChemSusChem* **2014**, *7*, 866−874.
(19) Yoon, Y.; Hall, A. S.; Surendranath, Y. Tuning of Silver Catalyst Mesostructure Promotes Selective Carbon Dioxide Conversion into Fuels. *Angew. Chem., Int. Ed.* **2016**, *55*, 15282−15286.
(20) Ma, S.; Luo, R.; Gold, J. I.; Yu, A. Z.; Kim, B.; Kenis, P. J. A. Carbon Nanotube Containing Ag Catalyst Layers for Efficient and Selective Reduction of Carbon Dioxide. *J. Mater. Chem. A* **2016**, *4*, 8573−8578.
(21) Ma, M.; Trzesniewski, B. J.; Xie, J.; Smith, W. A. Selective and Efficient Reduction of Carbon Dioxide to Carbon Monoxide on Oxide-Derived Nanostructured Silver Electrocatalysts. *Angew. Chem., Int. Ed.* **2016**, *55*, 9748−9752.
(22) Lu, Q.; Rosen, J.; Zhou, Y.; Hutchings, G. S.; Kimmel, Y. C.; Chen, J. G. G.; Jiao, F. A selective and efficient electrocatalyst for carbon dioxide reduction. *Nat. Commun.* **2014**, *5*, 3242.
(23) Salehi-Khojin, A.; Jhong, H. R. M.; Rosen, B. A.; Zhu, W.; Ma, S.; Kenis, P. J. A.; Masel, R. I. Nanoparticle Silver Catalysts That Show Enhanced Activity for Carbon Dioxide Electrolysis. *J. Phys. Chem. C* **2013**, *117*, 1627−1632.
(24) Martin, A. J.; Larrazabal, G. O.; Perez-Ramirez, J. Towards Sustainable Fuels and Chemicals through the Electrochemical Reduction of CO_2: Lessons from Water Electrolysis. *Green Chem.* **2015**, *17*, 5114−5130.
(25) Hernandez, S.; Farkhondehfal, M. A.; Sastre, F.; Makkee, M.; Saracco, G.; Russo, N. Syngas Production from Electrochemical Reduction of CO_2: Current Status and Prospective Implementation. *Green Chem.* **2017**, *19*, 2326−2346.
(26) Weiss, R. F. Carbon Dioxide in Water and Seawater: The Solubility of a Non-Ideal Gas. *Mar. Chem.* **1974**, *2*, 203−215.
(27) Schwarz, H. A.; Dodson, R. W. Reduction Potentials of CO_2- and the Alcohol Radicals. *J. Phys. Chem.* **1989**, *93*, 409−414.
(28) Chandrasekaran, K.; Bockris, J. O. In situ Spectroscopic Investigation of Adsorbed Intermediate Radicals in Electrochemical Reactions - CO_2- on Platinum. *Surf. Sci.* **1987**, *185*, 495−514.
(29) Whipple, D. T.; Finke, E. C.; Kenis, P. J. A. Microfluidic Reactor for the Electrochemical Reduction of Carbon Dioxide: The Effect of pH. *Electrochem. Solid-State Lett.* **2010**, *13*, B109.
(30) Endrődi, B.; Bencsik, G.; Darvas, F.; Jones, R.; Rajeshwar, K.; Janáky, C. Continuous-Flow Electroreduction of Carbon Dioxide. *Prog. Energy Combust. Sci.* **2017**, *62*, 133−154.
(31) Rosen, B. A.; Salehi-Khojin, A.; Thorson, M. R.; Zhu, W.; Whipple, D. T.; Kenis, P. J. A.; Masel, R. I. Ionic Liquid-Mediated Selective Conversion of CO_2 to CO at Low Overpotentials. *Science* **2011**, *334*, 643−644.
(32) Singh, M. R.; Kwon, Y.; Lum, Y.; Ager, J. W.; Bell, A. T. Hydrolysis of Electrolyte Cations Enhances the Electrochemical Reduction of CO_2 over Ag and Cu. *J. Am. Chem. Soc.* **2016**, *138*, 13006−13012.
(33) Thorson, M. R.; Siil, K. I.; Kenis, P. J. A. Effect of Cations on the Electrochemical Conversion of CO_2 to CO. *J. Electrochem. Soc.* **2013**, *160*, F69−F74.
(34) Verma, S.; Lu, X.; Ma, S.; Masel, R. I.; Kenis, P. J. A. The Effect of Electrolyte Composition on the Electroreduction of CO_2 to CO on Ag Based Gas Diffusion Electrodes. *Phys. Chem. Chem. Phys.* **2016**, *18*, 7075−7084.
(35) Kim, B.; Ma, S.; Jhong, H. R. M.; Kenis, P. J. A. Influence of Dilute Feed and pH on Electrochemical Reduction of CO_2 to CO on Ag in a Continuous Flow Electrolyzer. Electrochim. *Electrochim. Acta* **2015**, *166*, 271−276.
(36) Hafez, I. H.; Berber, M. R.; Fujigaya, T.; Nakashima, N. Enhancement of Platinum Mass Activity on the Surface of Polymer-wrapped Carbon Nanotube-Based Fuel Cell Electrocatalysts. *Sci. Rep.* **2015**, *4*, 6295.
(37) Fujigaya, T.; Nakashima, N. Fuel Cell Electrocatalyst Using Polybenzimidazole-Modified Carbon Nanotubes As Support Materials. *Adv. Mater.* **2013**, *25*, 1666−1681.
(38) Jhong, H. R. M.; Tornow, C. E.; Kim, C.; Verma, S.; Oberst, J. L.; Anderson, P. S.; Gewirth, A. A.; Fujigaya, T.; Nakashima, N.; Kenis, P. J. A. Gold Nanoparticles on Polymer-Wrapped Carbon Nanotubes: An Efficient and Selective Catalyst for the Electroreduction of CO_2. *ChemPhysChem* **2017**, *18*, 3274−3279.
(39) Fujigaya, T.; Kim, C.; Hamasaki, Y.; Nakashima, N. Growth and Deposition of Au Nanoclusters on Polymer-wrapped Graphene and Their Oxygen Reduction Activity. *Sci. Rep.* **2016**, *6*, 21314.
(40) Jhong, H. R.; Brushett, F. R.; Kenis, P. J. A. The Effects of Catalyst Layer Deposition Methodology on Electrode Performance. *Adv. Energy. Mater.* **2013**, *3*, 589−599.
(41) Ma, S.; Luo, R.; Moniri, S.; Lan, Y.; Kenis, P. J. A. Efficient Electrochemical Flow System with Improved Anode for the Conversion of CO_2 to CO. *J. Electrochem. Soc.* **2014**, *161*, F1124−F1131.
(42) Wuttig, A.; Yaguchi, M.; Motobayashi, K.; Osawa, M.; Surendranath, Y. Inhibited Proton Transfer Enhances Au-Catalyzed CO_2-to-Fuels Selectivity. *Proc. Natl. Acad. Sci. U. S. A.* **2016**, *113*, E4585−E4593.
(43) Frumkin, A. N.; Petrii, O. A.; Damaskin, B. B. Potentials of Zero Charge. In *Comprehensive Treatise of Electrochemistry*; Springer: Boston, MA, 1980.
(44) Katsounaros, I.; Chen, T.; Gewirth, A. A.; Markovic, N. M.; Koper, M. T. M. Evidence for Decoupled Electron and Proton Transfer in the Electrochemical Oxidation of Ammonia on Pt(100). *J. Phys. Chem. Lett.* **2016**, *7*, 387−392.
(45) Koper, M. T. M. Theory of Multiple Proton-Electron Transfer Reactions and its Implications for Electrocatalysis. *Chem. Sci.* **2013**, *4*, 2710−2723.
(46) Shi, C.; Chan, K.; Yoo, J. S.; Norskov, J. K. Barriers of Electrochemical CO_2 Reduction on Transition Metals. *Org. Process Res. Dev.* **2016**, *20*, 1424−1430.
(47) Tse, E. C. M.; Hoang, T. T. H.; Varnell, J. A.; Gewirth, A. A. Observation of an Inverse Kinetic Isotope Effect in Oxygen Evolution Electrochemistry. *ACS Catal.* **2016**, *6*, 5706−5714.
(48) Gomez-Gallego, M.; Sierra, M. A. Kinetic Isotope Effects in the Study of Organometallic Reaction Mechanisms. *Chem. Rev.* **2011**, *111*, 4857−4963.
(49) Conway, B. E.; Salomon, M. J. Studies on the Hydrogen Evolution Reaction Down to —150°C and the Role of Proton Tunneling. *J. Chem. Phys.* **1964**, *41*, 3169−3177.
(50) Krishtalik, L. I. Kinetic Isotope Effect in the Hydrogen Evolution Reaction. *Electrochim. Acta* **2001**, *46*, 2949−2960.
(51) Hatsukade, T.; Kuhl, K. P.; Cave, E. R.; Abram, D. N.; Jaramillo, T. F. Insights into the Electrocatalytic Reduction of CO_2 on Metallic Silver Surfaces. *Phys. Chem. Chem. Phys.* **2014**, *16*, 13814−13819.

DOI: 10.1021/acsenergylett.7b01096
ACS Energy Lett. 2018, 3, 193−198